

DEVELOPMENT STATUS OF INDIGENOUS COMPUTATIONAL FLUID DYNAMICS SOFTWARE FOR ARBITRARY COMPLEX GEOMETRY

K. C. Ng, M. Z. Yusoff, T. F. Yusaf and I. Hussein

Department of Mechanical Engineering, College of Engineering, Universiti Tenaga Nasional,
Jalan Kajang-Puchong, 43009 Kajang, Selangor Darul Ehsan

ABSTRACT

This paper describes the development status of an indigenous Computational Fluid Dynamics (CFD) software (FLOWSIM) capable of handling complex geometry. It addresses the development of the pre-processor, post-processor as well as the flow solvers that can handle a wide range of computational meshes. The flow solvers employ the second-order accurate cell vertex Finite Volume Method for space discretisation and multi-stage Runge-Kutta explicit time integration to solve the unsteady Reynolds Averaged Navier-Stokes (RANS) equations, where its unstructured counterparts are integrated with the commercial pre- and post-processor; it is time-effective and the range of simulations that can be attempted is extended towards complex geometry. Finally, the paper discusses the applications of this newly developed CFD software, together with the verification of results with predictions from commercial codes as well as experimental data..

Keywords : *Computational Fluid Dynamics, Coupled Solution Technique, Finite Volume Method, Indigenous CFD Codes, Navier-Stokes Equations*

1.0 INTRODUCTION

Numerical simulation on structural components has been widely accepted as the standard design tool in engineering applications. The concept of Computer Aided Design (CAD), Computer Aided Manufacturing (CAM) and more commonly, Computer Aided Engineering (CAE) provides an effective way in optimising the design of the final product. Nowadays, many numerical codes designed for structural analysis such as MSC-modules, ANSYS, COSMOS, LS-DYNA and IDEAS etc. have been integrated into the modern CAD systems in order to reduce the total design cycles, which is desired by a design engineer.

Apart from structural properties, characteristics of fluid flow, heat transfer as well as fluid-solid interaction may influence the performance and hence functionality of many products. In order to optimise the design, it is essential to include the modeling of fluid flow phenomena into numerical consideration. The art of predicting the flow characteristics numerically is called Computational Fluid Dynamics (CFD). Unfortunately, the development in this area has been much slower as compared to structural analysis - the fluid governing equations are embedded in a system of coupled non-linear Partial Differential Equations (PDE), which are more difficult to solve. In spite of this, the needs of the early aerospace community has driven the development of CFD in the sixties by integrating CFD techniques into the design of aircraft following the introduction of panel methods for subsonic flow [3,15] and the eighties have seen rapid developments in methods for solving the Euler and Navier-Stokes equations, such as the works published in [4,5,8,14]. More recently, [2,7] have applied the CFD techniques to the design of internal combustion engines and [12] in turbomachinery application. Increasingly CFD is becoming a crucial component in the design of industrial products and processes.

While commercial CFD software is vastly available and offered by numerous vendors such as FLUENT, CFDRC, AVL, CD-ADAPCO, etc, quite a number of companies continue to make substantial investments in the in-house development of CFD codes, such as TRANAIR at Boeing, TEAM at Lockheed, NEWT, BTOB3D and LOSS3D at Cambridge University, WIND at National Aeronautics and Space Administration (NASA), FLO- and FLO-MG series at Princeton University, etc., all of which have been used extensively in industrial applications. This renders that fluid flow is generally more complex than the behavior of structures [6] and customisable computational codes are hence desirable to predict the model-dependent fluid flow problems accurately since the predictions from commercially available CFD codes may sometimes be questionable particularly when flow complexity becomes apparent.

In local scenario, CFD has been applied in some areas of engineering on regular basis such as in PROTON, PERODUA, TNB Research, Johnson Medical and OYL Research and Development Center. However, no effort has been made to develop an indigenous CFD code and frequently foreign expertise is sought when using commercial software in engineering design and problem solving. This reflects that there is an urgent need to build this expertise locally by developing an indigenous CFD software that can be customised and modified by local industrial CFD users in accordance with their needs. Most importantly, it would lead to savings in foreign exchange.

A research group in Universiti Tenaga Nasional (UNITEN) is currently active in developing a fully local CFD software. The ultimate aim is to produce a low cost CFD software that can be used by local industry especially the Semi and Medium Scale Enterprises (SME). Nevertheless, the main objective of this paper is to describe the development status of this software and demonstrate its relevance in industrial applications, which

are geometrically sophisticated. The trend of development will be briefly discussed in Section 2.0 to dictate the emergence of each software modules in chronological order. A brief description of the numerical methods of the newly developed CFD software will be given in Section 3.0. The Graphical User Interfaces will be presented in Section 4.0. Finally, the accuracy of each CFD solvers will be verified with either the predictions from commercial code or experimental measurements, as demonstrated in Section 5.0. Section 6.0 concludes the current work.

2.0 THE TREND OF DEVELOPMENT

The idea is originated from [17], after the development of his structured two dimensional inviscid code for turbomachinery application. The original program was written in FORTRAN DOS environment and hence not user-friendly because it requires manual input of the input data and uses line command rather than window GUI-based user input. The decision is then made by including the window interface to the current solver so that the mesh generation, pre-processing, solver parameter set up and post-processing can be done easily. The developed GUIs for pre-processing and post-processing are called FLOWSIM-PRE and FLOWSIM-POST, respectively, which has been explained in details in [4]. To date, the solver has been upgraded in order to handle single-phase turbulent compressible flow with the inclusion of various turbulence models. The solver is called FLOWSIM-SQUAD2D and its application will be discussed in the following section.

Practically, fluid flows in three spatial dimensions. Therefore, the development of a 3D flow solver is found to be necessary. The first idea is to extend the existing 2D solver to become a 3D structured solver. It is easy, both in practicing and programming. The addressing issue in structured environment is straightforward due to the fact that the nodes are arranged in an orderly manner. It does have some disadvantages nevertheless. For example, one is restricted to use curved rectangles and this deteriorates the quality of the rectangles particularly in the vicinity of corners and sharp edges. Therefore, it is not suitable to be used in practical flow, where the flow domain is complicated enough in which structured meshing is impossible. Hence, it is novel to modify the existing solver to unstructured environment for flow simulation in complex domain becomes feasible. Unstructured hexahedral solver is then proposed and developed, namely FLOWSIM HEXA3D. By adopting the unstructured mesh generated by the commercial preprocessor of ANSYS, the current solver is capable to read the mesh connectivity in ANSYS format, with slight modification of the input deck to account for the control cards required by the solver. To visualise the flow variables, FIELDVIEW is chosen as the post-processor of the current unstructured solvers.

One may notice the limitation of hexahedral cells in handling geometry of arbitrary complexity. Although the hexahedral code is designed in an unstructured manner, difficulties may arise when one intends to mesh the flow domain that consist of sharp corners, surface twisting, intersection of two non-planar surfaces etc. One can fit the hexahedral elements into the flow domain while maintaining the quality of the mesh, however, the process takes time and hence it is not efficient in simulating practical flow. To solve the flow parameters in complex geometry, intense research has been carried out in the past few decades such as the

2D triangular flow solver developed in [10]. For 3D applications, it is a common practice for CFD engineers to mesh the entire flow domain using tetrahedral elements due to the fact that cells with triangular faces can be generated automatically in complex geometry by using the modern mesh generators. Having in mind that the plane with zero warpage is bounded by three nodes in 3D space, which is equivalent to the formation of a triangular face, hence, triangular elements and tetrahedral elements are commonly utilised in 2D and 3D flow environment, respectively in order to simulate practical flow. Subsequently, two triangular based solvers are developed, namely FLOWSIM-TRIA2D and FLOWSIM TETRA3D to handle 2D and 3D flows, respectively.

All the modules are then integrated into a single software unit called FLOWSIM.

The trend of development has been summarised in Table 1.

Table 1: The trend of development of FLOWSIM in chronological order

Modules	Type	Dimensionality	Pre-processor	Post-processor
FLOWSIM-PRE	Pre-processor	2D	-	-
FLOWSIM-POST	Post-processor	2D	-	-
FLOWSIM-SQUAD2D	Solver	2D	FLOWSIM-PRE	FLOWSIM-POST
FLOWSIM-HEXA3D	Solver	3D	ANSYS	FIELDVIEW
FLOWSIM-TRIA2D	Solver	2D	ANSYS	FIELDVIEW
FLOWSIM-TETRA3D	Solver	3D	ANSYS	FIELDVIEW

3.0 NUMERICAL FORMULATIONS

3.1 GOVERNING EQUATIONS

The three-dimensional continuity, x -, y - and z -momentum, energy, turbulent transport equations for turbulent kinetic energy (k) and its dissipation rate (ϵ) describing the flow of a compressible fluid expressed in strong conservation form in the x -, y - and z -Cartesian co-ordinate system may be written as: -

$$\frac{\partial W}{\partial t} + \frac{\partial F}{\partial x} + \frac{\partial G}{\partial y} + \frac{\partial H}{\partial z} = J \quad (1)$$

W represents the conserved variables whereas F , G and H are the overall fluxes in x -, y - and z - directions respectively, J is the source vector. The detailed formulations can be found in [13].

3.2 NUMERICAL SCHEMES

The flow domain is replaced by a finite number of grid points on a mesh system commonly known as H-mesh in FLOWSIM-SQUAD2D, unstructured hexahedral mesh in FLOWSIM-HEXA3D, unstructured triangular mesh in FLOWSIM-TRIA2D and unstructured tetrahedral mesh in FLOWSIM-TETRA3D. The governing equations are solved simultaneously (coupled solution technique) in their integral form for each compact stencil of finite volumes using time-marching method, as shown in Figure 1 for two-dimensional cases.

The spatial integration is performed using second-order accurate central discretisation. A blend of second-and-fourth order artificial dissipations with pressure switch is added to the residuals prior to the time integration to remove wiggles from the solution. The temporal integration is done using the second-order accurate, 4-stage Runge-Kutta time-stepping method proposed by [4]. To speed up the convergence, 3

types of convergence acceleration schemes are employed: local time stepping, enthalpy damping for inviscid simulation and implicit residual averaging. At inlet boundary, the total pressure, total temperature and flow angle are fixed while the static pressure is extrapolated from the interior if the inflow is subsonic. Otherwise, all the variables will be specified. At exit, if the exit flow is subsonic, only the static pressure is fixed, while total pressure, total temperature and flow angle are extrapolated from the interior. If the exit flow is supersonic, all four variables are extrapolated from the interior.

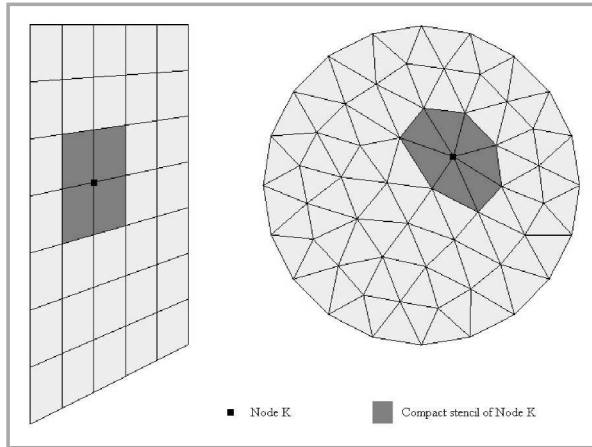


Figure 1: Compact stencil in 2D mesh environment: H-mesh (left) and triangular mesh (right)

At the solid boundary, no slip condition is used. The turbulence transport equations are integrated in exactly the same way. Due to the non-linear source terms in k - ϵ equations, it is well known that the k - ϵ equations are instability prone during the transitory phase of the computations particularly at nodes near the wall due to the high gradients of k and ϵ . In order to stabilise the computations of k and ϵ , they are bounded by suitable limiters suggested in [1]. On solid walls, k and ϵ are set to 0. For nodes adjacent to the wall, wall functions are introduced.

4.0 GRAPHICAL USER INTERFACES (GUI)

4.1 FLOWSIM-PRE

The GUI for the 2D structured solver (FLOWSIM-SQUAD2D) is designed using MATLAB. Generally, the features are categorised into 'Pages', being arranged in accordance to the CFD-modeling hierarchy, starting from the first step of CFD modeling process (geometry creation) to the activation of the flow solver.

Figure 2 shows the GUI for FLOWSIM-PRE, which is the pre-processor of the authors' structured 2D solver, namely FLOWSIM-SQUAD2D. It consists of 4 main parts: the Graphics Window, which displays the geometry and the mesh, the Control Panel, the Page Panel and the Command Panel. The appearance of Command Panel changes in accordance to the Page Panel selection. The Page Panel consists of: -

- File Page - The main page of FLOWSIM-PRE, this page is designed to transfer all the geometrical and mesh data specified by the user to an input file.
- Fluid Page – Set the fluid properties such as specific heat capacity, gas constant, specific heat ratio, Prandtl no,

viscosity etc. Selection of simulation type such as inviscid or viscous flow is available.

- Boundary Conditions Page – Set the inlet and outlet boundary conditions.
- Control Card Page – Set up of numerical constants such as iteration number, time step factor, turbulence control parameters, artificial viscosity coefficients, and convergence acceleration schemes.
- Solver Page – Initiate the solver and convergence plot.

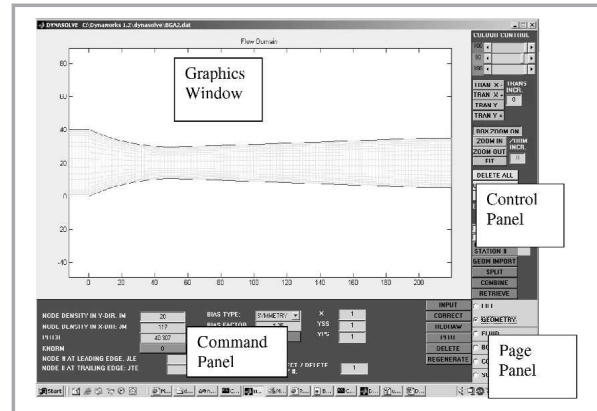


Figure 2: FLOWSIM-PRE user interface

4.2 FLOWSIM-POST

Figure 3 illustrates the GUI for FLOWSIM-POST, the post-processor. Similar to the pre-processor, FLOWSIM-POST consists of 4 main parts. The Graphics Window is able to display up to a maximum of four windows to perform post-processing. It facilitates the user in viewing different plots in a single window. Also, window colour adjustment, plot translation as well as zooming operation are included in Control Panel. There are 2 pages available, which are FILE and POST. The post-processing routines that can be activated are line plot, mesh plot, velocity vector plot, line contours and fringe plots.

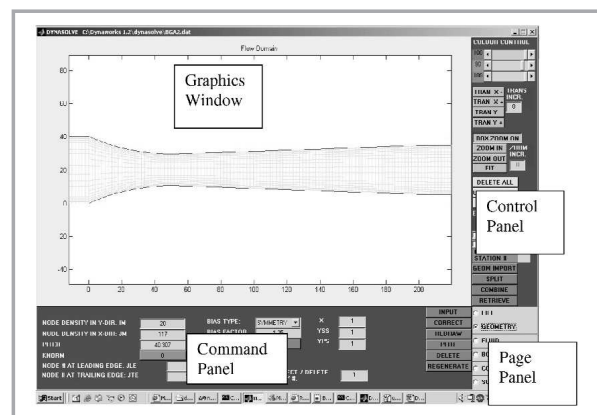


Figure 3: FLOWSIM-POST user interface

5.0 TEST CASES

The following sections will describe the applications of the software modules to various test cases.

5.1 FLOWSIM-SQUAD2D: Blade-to-Blade Calculations on a Turbine Nozzle Cascade

Blade-to-blade flow simulations on a turbine nozzle blade cascade are considered. The blade profile belongs to a stator of a low-pressure steam turbine. The geometry of the blade was generated using FLOWSIM-PRE, the pre-processor of the current solver. The experimental surface pressure measurements on the cascade were performed in [9].

Three flow cases at overall inlet total to outlet static, P_{inlet}/P_b , pressure ratios of 1.49, 1.83 and 2.32 were simulated. The overall pressure ratios of 2.32 correspond to supersonic outlet, while 1.83 corresponds to transonic outlet. The flow conditions with subsonic outlet are represented by tests at an overall pressure ratio of 1.49.

The mesh illustrated in Figure 4 consists of 33 x 230 grids. The mesh resolution near the wall is increased to account for the steep flow gradient within the boundary layer. A comparison of measured and calculated values of blade surface static pressure for subsonic, transonic and supersonic outflow conditions are presented in Figures 5, 6 and Figure 7, respectively. In general, the predicted surface pressure compares well with the experimental data, except for the pressure values near the trailing edge. This is due to the over-predicted turbulent viscosity in the flow passage since the employed turbulence model does not contain a description of streamline curvature on turbulence; in which limitation occurs when the model is used to predict turbulent flow in turbine blade passage involving highly curved boundary layer.

5.2 FLOWSIM-TRIA2D: Transonic Flow Past a RAE 2822 Airfoil

Next, the flow past a RAE 2822 airfoil is examined using the triangular solver. The mesh consists of 24891 triangles and 12645 nodes. The boundary layer is treated carefully by fitting structured quadrilateral grids near the wall region initially. Then, those quadrilateral grids will be split into triangles, as illustrated in Figure 8. The airfoil is tilted at an attack angle of 2.31° and it is cruising at a Mach number of about 0.73.

The flow is assumed to be fully laminar in this test case by merely solving the Navier-Stokes equations. The inflow is subsonic, being accelerated to supersonic speed of Mach 1.2 at approximately half chord distance downstream from the leading edge. A compression shock is formed; decelerating the flow to the free stream Mach number as can be observed in Figure 9(a). The predicted Mach number has been presented in its contour form and it shows good agreement with the simulation result predicted from the WIND code developed in National Aeronautics and Space Administration (NASA), as presented in Figure 9(b).

Figure 10 depicts the plot of pressure coefficient at upper and lower surface of the airfoil body as compared to the experimental data. The shock is clearly presented on the upper surface showing the discontinuity of static pressure data. A relatively constant pressure area can be observed at region upstream from the shock wave. In general, good agreement has been obtained.

5.3 FLOWSIM-HEXA3D: Transonic Compressor Rotor

In this section, the code is applied to the study of the three-dimensional flowfield in the axial flow single stage transonic

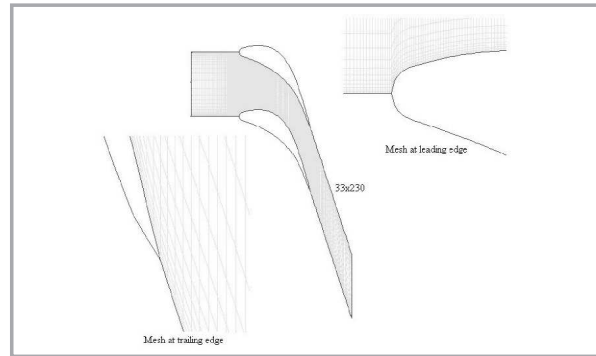


Figure 4: H-mesh used in the nozzle blade cascade

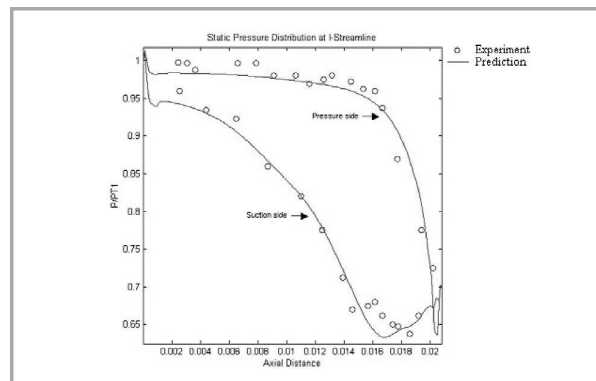


Figure 5: Blade surface pressure plot for the nozzle cascade during subsonic flow condition

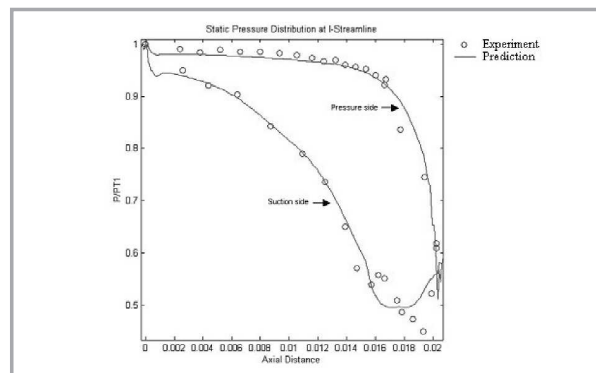


Figure 6: Blade surface pressure plot for the nozzle cascade during transonic flow condition

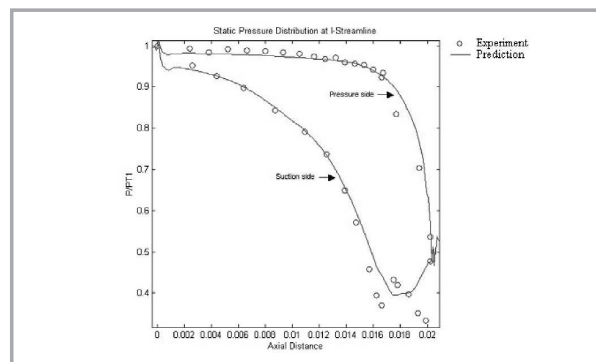


Figure 7: Blade surface pressure plot for the nozzle cascade during supersonic flow condition

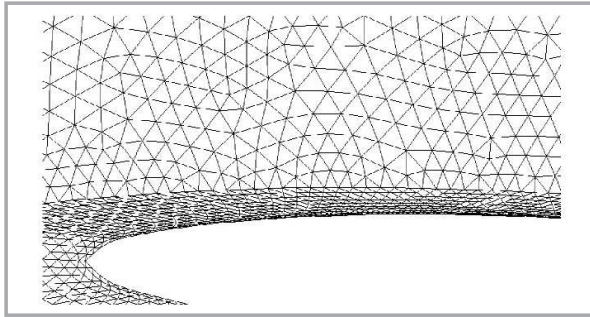


Figure 8: The mesh resolution near the airfoil body

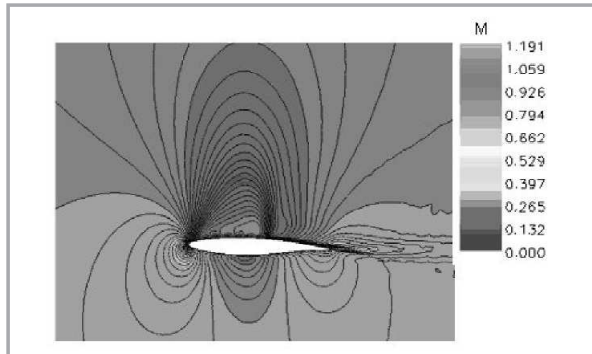


Figure 9a: Contour of Mach number predicted by FLOWSIM-TRIA2D

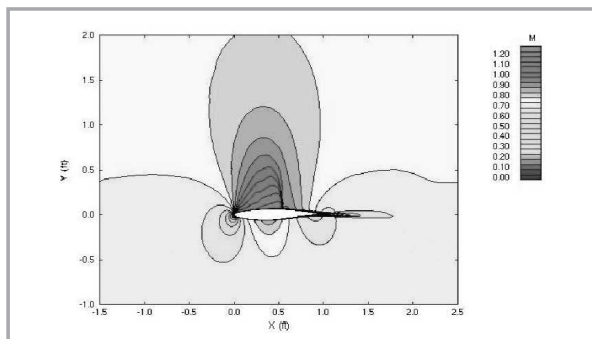


Figure 9b: Contour of Mach number predicted by WIND (NASA)
[Reproduced from Slater (2002)]

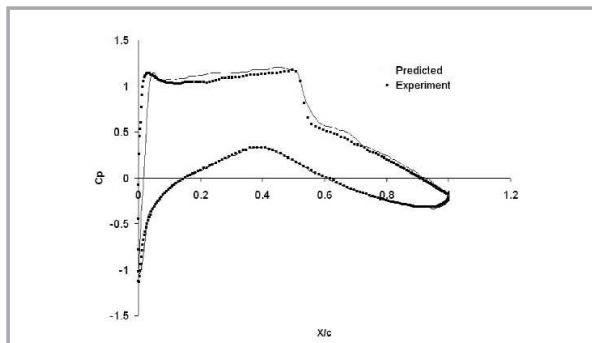


Figure 10: Comparison of pressure coefficient at the upper and lower surface of the airfoil

compressor rotor located at Deutsche Forschungsanstalt fur Luft und Raumfahrt (DFVLR). The objective here is to demonstrate the accuracy of FLOWSIM-HEXA3D as compared to the prediction from the commercial code CFX-5, which is prominent in the area of turbomachinery.

The compressor rotor has an inlet tip diameter of 0.4m, 28 blades per row, a hub-tip ratio of 0.5 and tip solidity of 1.34. The design mass flow rate is 17.1 kg/s rotating at 20260 rpm about the x-axis in clockwise direction. The mesh employed is relatively coarse, consisting of 13294 cells and 15228 nodes per flow passage with crude refinement in zone near to the casing, hub and blade. No attempt was performed to resolve the tip leakage flow. Similar mesh was used in both the present solver and CFX-5, as illustrated in Figure 12 showing the surface mesh of the complete DFVLR compressor rotor.

The flow equations were solved in rotating frame of reference with appropriate Coriolis and centripetal force terms and it was run until convergence. The relative inflow Mach number varies from around 0.7 to about 1.4 towards the casing. Figures 13, 14 and 15 illustrate the predicted relative Mach number at the blade-to-blade plane of $z=120\text{mm}$, $z=140\text{mm}$ and $z=150\text{mm}$, respectively. At $z=120\text{mm}$, the flow accelerates to just sonic near the leading edge and decelerates abruptly to Mach 0.5 across a shock wave. At $z=140\text{mm}$ and $z=150\text{mm}$, the relative inflow is supersonic and a well-resolved oblique shock forms at region slightly downstream of the leading edge as predicted by the current solver. Furthermore, current prediction reveals that there is another shock wave originating from the leading edge that comes into interaction with the internal flow field. CFX-5 tends to smear the leading-edge-shock, probably due to the excessive numerical diffusion inherited from the spatial differencing scheme. In general, by considering the coarseness of the mesh, the resolution of the shock pattern is found to be satisfactory.

Figures 16, 17 and 18 present the pressure distribution at the cross-flow plane of $x=0\text{mm}$, $x=-10\text{mm}$ and $x=5\text{mm}$, respectively and illustrate clearly the shock patterns between the rotating blades. At $x=-10\text{mm}$, two shock surfaces were predicted from the current solver as well as CFX-5: the first shock surface extends from the hub-suction surface corner to the casing, which corresponds to the leading-edge-shock and the second corresponds to the shock surface attached to the pressure side of the blade surface at slightly downstream from the leading edge. At $x=0\text{mm}$ and $x=5\text{mm}$, the shock surface causes a significance pressure drop from the pressure to suction blade surface, and impinges impinging the suction blade surface and the casing as predicted by the current solver. However, CFX-5 predicted the shock to be formed at slightly downstream and it is relatively smeared as compared with the shock representation by FLOWSIM-HEXA3D.

5.4 FLOWSIM-TETRA3D: Transonic Flow Past a DLRFR Aircraft

The last test case will demonstrate the ability of the software to simulate flows over complex geometry. Only inviscid simulation is performed to simulate the transonic flow past a DLRFR aircraft. The mesh consists of 206991 tetrahedral cells and 42406 nodes. No special treatment is done on the mesh resolution near the aircraft body region. The inlet Mach number is about 0.73 and the problem is run in a serial machine (Pentium 4, 2.8 GHz) until convergence.

The colour plot of static pressure predicted by the current solver is presented in Figure 19. Comparison is done with the result predicted by CFD++, as illustrated in Figure 20. Contrary to the current flow solver, turbulent flow simulation is done in CFD++ environment, consisting of 5 million hexahedral cells

with $y=25$ at the first centroid away from the walls. However, some essential flow physics can still be captured using the current flow solver, such as stagnation flow near the nose and the leading edge of the wing. Also, observation shows that there is a shock wave impinges at approximately half-width of the wing body. Surprisingly, by considering the coarseness of the mesh employed in the current solver, the shock wave can still be captured without employing any mesh adaptation algorithm. No experimental data is available for this problem. However, by comparing the results obtained from the two different solvers, the agreement is encouraging.

6.0 CONCLUSION AND FURTHER WORK

The status of indigenous CFD software development in Universiti Tenaga Nasional has been presented. A range of

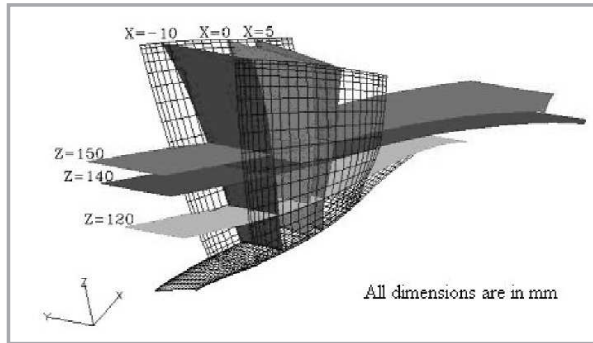


Figure 11: The location of the cutting planes established for the presentation of results

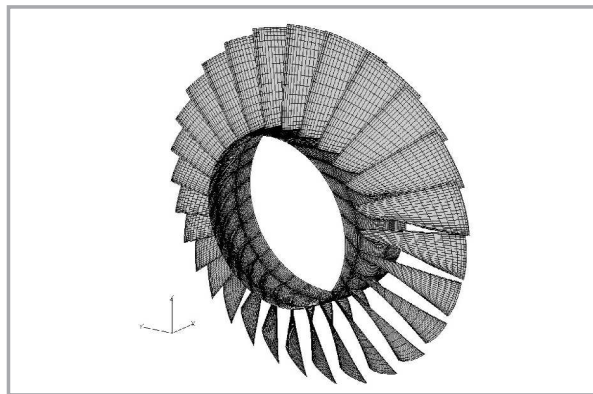


Figure 12: Surface mesh for the DFVLR compressor rotor

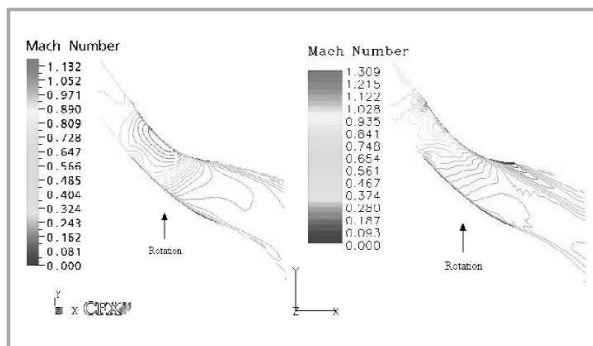


Figure 13: Comparisons of relative Mach contours at $z=120\text{mm}$ using CFX-5 (left) and FLOWSIM-HEXA3D (right)

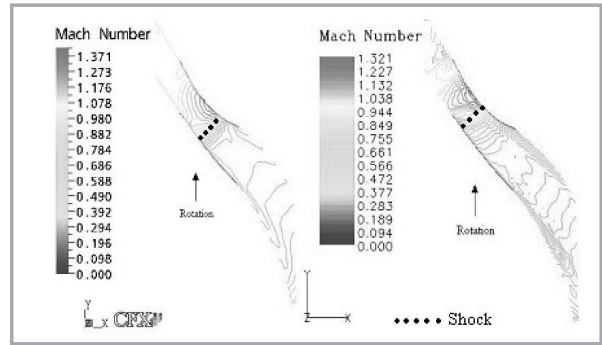


Figure 14: Comparisons of relative Mach contours at $z=140\text{mm}$ using CFX-5 (left) and FLOWSIM-HEXA3D (right)

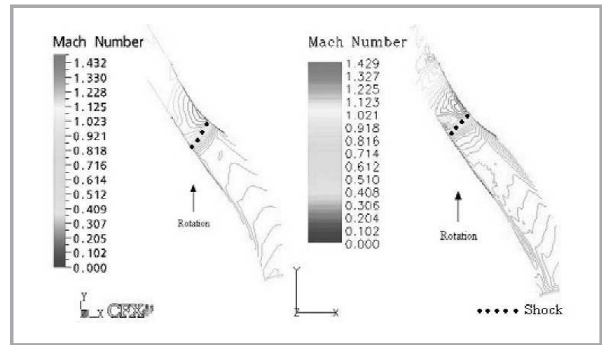


Figure 15: Comparisons of relative Mach contours at $z=150\text{mm}$ using CFX-5 (left) and FLOWSIM-HEXA3D (right)

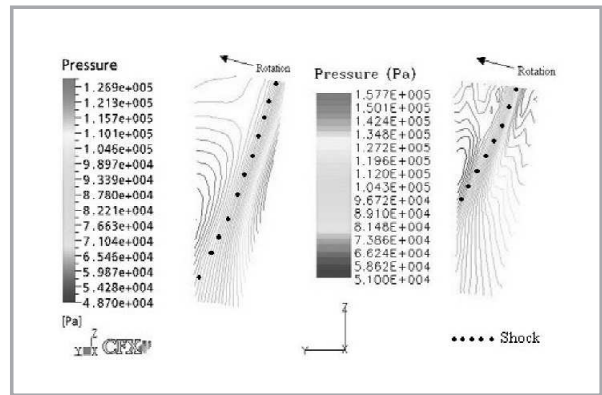


Figure 16: Comparisons of static pressure contours at $x=0.0\text{ mm}$ using CFX-5 (left) and FLOWSIM-HEXA3D (right)

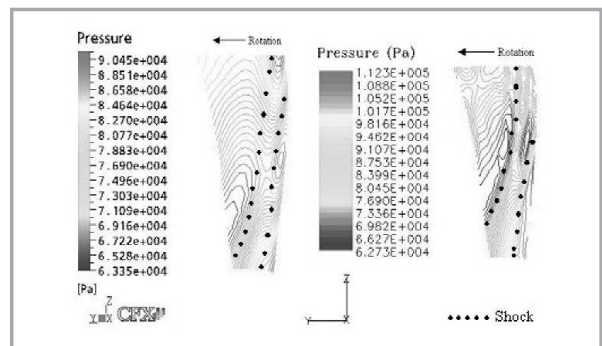


Figure 17: Comparisons of static pressure contours at $x=-10.0\text{ mm}$ using CFX-5 (left) and FLOWSIM-HEXA3D (right)

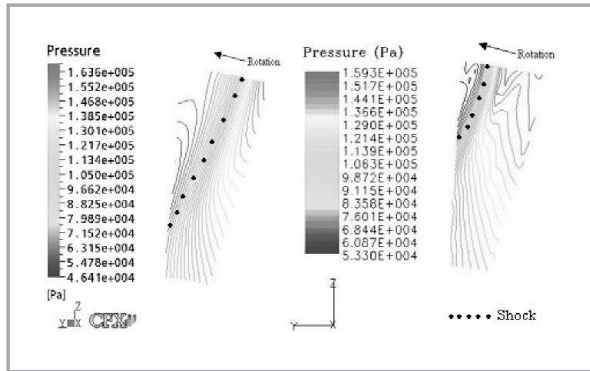


Figure 18: Comparisons of static pressure contours at $x=5.0$ mm using CFX-5 (left) and FLOWSIM-HEXA3D (right)

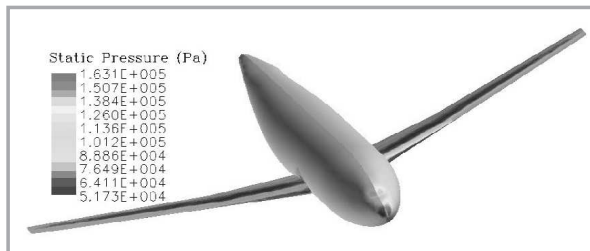


Figure 19: Static pressure distribution predicted by FLOWSIM-TETRA3D

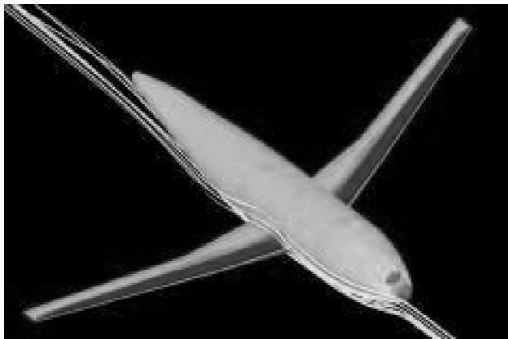


Figure 20: Static pressure distribution predicted by CFD++ [Reproduced from Metacomp Technologies]

single-phase compressible flow solvers that handle structured and unstructured meshes has been developed, together with the Graphical User Interfaces (GUI) for the 2D structured solver. The results have been compared with experimental data as well as commercial codes and reasonably good agreements have been achieved, even in flow cases that are geometrically complex. However, the solution is susceptible to wiggles in certain flow region due to the embedded character of the current differencing scheme. In order to overcome this problem, high-resolution differencing scheme is currently being implemented on the flow solvers. Further development of the software will be the incorporation of implicit time-marching scheme, multigrid convergence accelerator and pseudo-compressibility factor to simulate incompressible flow using the present coupled solution technique.

ACKNOWLEDGEMENTS

This project is funded by the Ministry of Science Technology and Innovation (MOSTI), Malaysia under the

IRPA Grant No. 09-99-03-0013-EA001 and UNITEN Internal Research Grant No. J510010026. ■

REFERENCES

- [1] Dawes, W.N. (1992), "The Solution-Adaptive Numerical Simulation of the 3D Viscous Flow in the Serpentine Coolant Passage of a Radial Inflow Turbine", ASME Gas Turbine Conference, Cologne.
- [2] Gosman, A.D.; Ghobadian, A.; Jasak, H.; Kaludjeric, B. and Lee, F. (1999), "Prediction of Engine and Furnace Combustion using Advanced CFD and Computing Methodology", Proceedings of the Asia-Pacific Conference on Combustion, Taiwan.
- [3] Hess, J.L. and Smith, A.M. (1962), "Calculation of Non-Lifting Potential Flow about Arbitrary Three-Dimensional Bodies", Douglas Aircraft Report, ES 40622, 1962.
- [4] Jameson, A., Schmidt, W. and Turkel, E. (1981), "Numerical Solutions of the Euler Equations by Finite Volume Methods using Runge-Kutta Time Stepping Schemes", AIAA Paper No. 81-1259.
- [5] Jameson, A., Baker and Timothy, J. (1983), "Solution of the Euler Equations for Complex Configurations", Proc. AIAA 6th Computational Fluid Dynamics Conference, Danvers, pp293-302.
- [6] Jameson, A., Martinelli, L., Alonso, J., Vassberg, J. and Reuther, J. (2000), "Perspectives on Simulation Based Aerodynamic Design", Proceedings of a Symposium Honoring Prof. Satofuka on the Occasion of his 60th Birthday, Kyoto, Japan, 15-17 July, 2000.
- [7] Jasak, H., Luo, J.Y., Kaludjeric, B.; Gosman, A.D.; Echtele, H. Liang, Z., Wirbeleit, F., Wierse, M.; Rips, S., Werner, A., Fernstrom, G. and Karlsson, A. (1999), "Rapid CFD Simulation of Internal Combustion Engines", SAE World Congress, Detroit.
- [8] MacCormack, R.W. (1985), "Current Status of Numerical Solutions of the Navier-Stokes Equations", AIAA Paper 85-0032, AIAA 23rd Aerospace Sciences Meeting, Reno.
- [9] Mamat, Z.A. (1996), "The Performance of a Cascade of Nozzle Turbine Blading in Nucleating Steam", Ph.D. Thesis, University of Birmingham.
- [10] Mavriplis, D.J. and Jameson, A. (1990), "Multigrid Solution of the Navier Stokes Equations on Triangular Meshes", AIAA Journal Vol. 28, No. 8.
- [11] Metacomp Technologies, "DLR-F4, CFD++ Solution Gallery", Internet: http://www.metacomptech.com/cfd++/gallery_DLR.html

- [12] Ng, K.C. and Yusoff, M.Z. (2004), "Development of User-Friendly 2D CFD Software for Teaching Fluid Dynamics: FLOWSIM", Final Report of UNITEN Research Project No. J510010026, Universiti Tenaga Nasional, May 2004.
- [13] Ng, K.C., Yusoff, M.Z. and Yusaf, T. (2005), "Numerical Simulation of 3D Transonic Flow in a Compressor Rotor", Accepted for publication in International Journal of Simulation and Modeling.
- [14] Pulliam, T.H., and Steger, J.L. (1985), "Recent Improvements in Efficiency, Accuracy and Convergence for Implicit Approximate Factorization Algorithms", AIAA Paper 85-0360, AIAA 23rd Aerospace Sciences Meeting, Reno.
- [15] Rubbert, P.E. and Saaris, G.R. (1968), "A General Three Dimensional Potential Flow Method Applied to V/STOL Aerodynamics", SAE Paper 680304.
- [16] Slater, J.W. (2002), "RAE 2822 Transonic Airfoil: Study #4", NASA Glenn Research Centre, Ohio. Internet: <http://www.grc.nasa.gov/WWW/wind/valid/raetaf/raetaf04/raetaf04.html>
- [17] Yusoff, M.Z. (1998), "A Two-Dimensional Time-Accurate Euler Solver for Turbomachinery Applications", Journal of the Institution of Engineers, Malaysia, Vol. 59, No.3.

PROFILES



Mr. Ng Khai Ching

He is currently working as Research Assistant in Department of Mechanical Engineering, Universiti Tenaga Nasional (UNITEN), Malaysia. He obtained his BEng. in Mechanical Engineering from UNITEN in 2003. His current research interests are Computational Fluid Dynamics (CFD), numerical computing and CAE software development.



Dr Mohd. Zamri Yusoff

He is currently the Deputy Dean of the College of Engineering, UNITEN. He obtained his PhD in Mechanical Engineering from the University of Birmingham, UK in 1997. His research interests are in CFD, numerical modeling, condensation and other energy related studies.



Dr Talal Yusaf

Dr. Talal Yusaf is currently the Associate Professor in UNITEN. He obtained his PhD in Mechanical Engineering from Universiti Kebangsaan Malaysia (UKM), Malaysia. His areas of specializations are biotechnology and combustion.

ANNOUNCEMENT

First Bulletin / Call for Papers National Food Production and Processing Conference

Theme – Towards Malaysia as a Major Food

Exporter: Challenges

23 - 24 August 2006
Equatorial Hotel, Bangi
Selangor Darul Ehsan

Organised by : IEM, AFETD
Sponsored by : MARDI, MSAE, MOA, UPM

Conference Session

- Session 1 :** Globalisation and opportunities for the Malaysian food industry
Session 2 : Food Production Technology
Session 3 : Food Processing Technology
Session 4 : Panel Discussions – Engineering Contributions to Meeting the Challenges

Call for Papers & Poster Papers

The conference shall take the format of invited speakers, submitted papers for oral presentation, poster sessions and a forum. Interested paper presenters are invited to submit paper in subject matters related to the theme of the conference. An abstract of the paper title of about 300 words double spaced on an A4 paper, should be mailed or e-mailed to the conference secretariat. The abstract shall include the author's names, organisation address and telephone, fax, e-mail contacts. If hardcopy is given, 5 copies would be required. E-mail or softcopy is encouraged.

Important Dates

Submission/Acceptance of Abstracts by : **1 May 2006**
Submission of Full Papers by : **30 June 2006**
Submission of Final Manuscripts for Publication of Proceedings by : **31 July 2006**

Conference Language

The language of the Conference shall be English.

Accommodation

Participants are to arrange accommodations on their own. A list of hotels in KL, Seri Kembangan, Kajang, Putrajaya and Cyberjaya will be available on request to the secretariat.

Registration Fees

The registration fee for the two-day conference shall be:

IEM Members	: RM 400
Graduate Members	: RM 300
Non-IEM Members	: RM 500
Students	: RM 200

This shall include a copy of the proceedings, four tea break refreshments and two lunches. The conference shall be accredited with 16 CPD-HRS for professional engineers.

Enquiries

All enquiries, correspondences, registration and payments are to be forwarded to the:

Conference Secretariat

NFPPC,
The Institution of Engineers, Malaysia
Bangunan Ingenieur, Lots 60-62, Jalan 52/4
P.O. Box (Jalan Sultan)
46720 Petaling Jaya
SELANGOR DARUL EHSAN
Tel : 03-7968 4001 / 4002
Fax : 03-7957 7678
E-Mail: sec@iem.org.my
Website : <http://iem.org.my/afetd.afehome.htm>